



Diagnosis of Delaminated Composites Using Post-processed Strain Measurements under Impact Loading

K. Askaripour*, M. J. Fadaee

Department of Civil Engineering, Shahid Bahonar University of Kerman, Kerman, Iran

PAPER INFO

Paper history:

Received 20 November 2018

Received in revised form 21 December 2018

Accepted 03 January 2019

Keywords:

Composite

Delamination Identification

Dynamic Strain

Impact

ABSTRACT

Potentially having a destructive influence on the mechanical properties of composite laminates, the invisible phenomenon of delamination frequently occurs under impact loading. In the present study, simulating the performance of long-gauge fiber Bragg grating sensors, impact-induced average strains within laminated composites are utilized to develop a delamination identification technique. First, strain-based modal parameters are extracted from the estimator of frequency response functions using two different approaches. Next, these parameters are employed in various damage detection indicators. Then, the presence, location, and severity of delamination introduced at locations with the least effect on modal changes are detected. The results of different numerical examples with various delamination sizes and positions elucidate the considerable efficiency of average-strain measurements to diagnose delaminated composites.

doi: 10.5829/ije.2019.32.01a.07

1. INTRODUCTION

Diagnosis of the structural integrity of laminated composites has become one of the most dynamic research fields in engineering. Laminated composites have found a special place in various industries due to their selective properties, particularly the high ratio of stiffness to mass. The mechanical behavior of such structures and their reaction under loading compared to conventional isotropic structures such as steel are different [1]. For instance, impact or repeated cyclic stresses may cause layers to be separated at interfaces of each two layers, which is known as delamination phenomenon [2, 3]. Up to 60 % of the material's initial stiffness can be consumed by delamination development. Therefore, extensive research regarding delamination detection has been conducted.

Employing the degradation of material properties, vibration-based techniques are among the most commonly used techniques for delamination detection. Frequency shifts along with the graphical, artificial neural network, and surrogate assisted optimization techniques have been studied for this purpose in

composite beams [4]. The effects of delamination on modal frequency variations within composite beams in the presence of a concentrated mass loading have been investigated [5]. Some other studies employing vibration-based techniques for the inverse problem of the delamination detection are reported in literature [6–7]. Above review clarifies that frequency responses in spite of requiring further processing have attracted many researchers. However, modal shapes measured via long-gauge strain fiber Bragg grating (FBG) sensors are more efficient parameters.

Average-strain measurements obtained by multiplexing capability of long-gauge FBG sensors have the unique merit of reflecting both local and global information of a structure. The issues related to the application of long-gauge FBG technique for health monitoring of steel structures have been investigated through theoretical modal analysis [8]. The macro-strain based modal parameters are useful in detecting damaged steel elements [9]. Literature review implies that the idea of average strains of FBG sensors has not been applied to delaminated composites. While evaluating the performance of the boundary conditions of delamination and of the impact location, average strains are global responses to develop a less time-consuming

*Corresponding Author: askaripour@eng.uk.ac.ir (K. Askaripour)

diagnosis technique. A different way for obtaining strain frequency function matrix is embedded into the diagnosis technique.

The objectives of the present study are to extract average-strain measurements under impact loading applying the dynamic analysis in the presence of delamination and to investigate delamination identification using processed average strains. To that end, first, composite laminates with delamination of different lengths at various axial locations and layer interfaces are modeled to obtain structural properties. Details of modeling in Abaqus are provided in section 2. Next, as mentioned in section 3, obtained structural properties converted into MATLAB are analyzed through the dynamic Bathe method under impact, and structural responses are extracted. Then, section 4 deals with structural responses to develop a new delamination identification technique. Afterward, two damage identification indicators are provided in section 5 and different numerical examples are included to verify the efficiency of the proposed delamination identification technique in section 6. Finally, the study is concluded in section 7.

2. MODELING DETAILS

The finite element (FE) software Abaqus has been used to model delaminated composites. Frequency analysis is performed to find the mass and stiffness matrices fed into the Bathe method. The implicit Bathe method in MATLAB is employed to obtain displacements and rotations under impact loading. The results are also validated with those obtained from Abaqus employing implicit dynamic analysis.

Displacements as a function of x , y and z (in-plane axial and transversal coordinates, and the coordinate normal to the plate, respectively) at any point in FSDT theory for the intact shell are computed as follows:

$$u = u^0 - z \partial w^0 / \partial x; v = v^0 - z \partial w^0 / \partial y; w = w^0 \quad (1)$$

where u^0 , v^0 and w^0 (a function of x and y) on the right-hand side are the mid-surface displacements in three specified directions; z is the distance between mid-surface and each other arbitrary surface; and $\partial w^0 / \partial x = \psi(x)$ and $\partial w^0 / \partial y = \psi(y)$ are rotations [10].

Single-layer shell elements can be utilized in FE analysis of an intact laminate, while double-layer shell elements attached by two connection modes will be employed for delaminated regions in a delaminated laminate. Therefore, delaminated composite laminates are modeled by employing single and double-layer shell elements in the intact and delaminated regions, respectively (shown in Figure 1). Connecting upper and lower sub-laminates of double-layer shell elements is

conducted by either free mode or constrained mode [11]. To tie the upper and lower sub-laminates in the constrained mode, the following equation (at e.g., x -direction) according to Equation (1) is employed:

$$u^{1,0} - (h_1/2)(\partial w^{1,0} / \partial x) = u^{2,0} + (h_2/2)(\partial w^{2,0} / \partial x) \quad (2)$$

where the superscripts 1 and 2, and h_1 and h_2 refer to the upper and lower sub-laminates and their thicknesses, respectively. Displacements, as well as rotations of all three nodes of the upper and lower sub-laminates and the intact region at the borders between the delaminated and intact regions (interface region) are also tied in both the free and constrained modes.

Data transfer process includes the export operation of the stiffness and mass matrices along with node numbers from Abaqus and the import operation of these data into MATLAB. Accordingly, a code is programmed in MATLAB.

3. DYNAMIC ANALYSIS

Having the mass and stiffness matrices in full format and applying impact loading, the implicit Bathe method, as an accurate numerical method compared to other available ones, is used in MATLAB to extract the responses required for further analyses [12]. Therefore, the following equations are programmed:

$$\hat{K}_1^{t+\Delta t/2} X = \hat{F}_1; \hat{K}_2^{t+\Delta t/2} X = \hat{F}_2. \quad (3)$$

where

$$\hat{K}_1 = \frac{16}{\Delta t^2} M + \frac{4}{\Delta t} C + K; \hat{K}_2 = \frac{9}{\Delta t^2} M + \frac{3}{\Delta t} C + K \quad (4)$$

$$\hat{F}_1 = {}^{t+\Delta t/2} F + M \left(\frac{16}{\Delta t^2} {}^t X + \frac{8}{\Delta t} {}^t \dot{X} + \frac{3}{\Delta t^2} {}^t \ddot{X} \right) + C \left(\frac{4}{\Delta t} {}^t X + {}^t \dot{X} \right) \quad (5)$$

$$\hat{F}_2 = {}^{t+\Delta t} F + M \left(\frac{12}{\Delta t^2} {}^{t+\Delta t/2} X - \frac{3}{\Delta t^2} {}^t X + \frac{4}{\Delta t} {}^{t+\Delta t/2} \dot{X} - \frac{1}{\Delta t} {}^t \dot{X} \right) + C \left(\frac{4}{\Delta t} {}^{t+\Delta t/2} X - \frac{1}{\Delta t} {}^t X \right). \quad (6)$$

in which M , C , K , and F are the mass, damping, stiffness matrices obtained from section 2, and the impact loading vector.

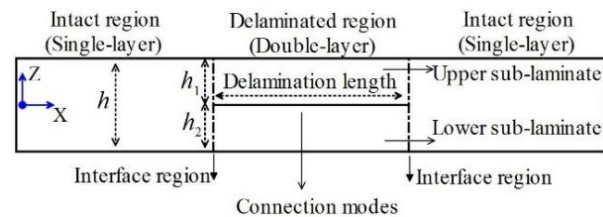


Figure 1. Modeling delaminated composite laminate

The responses including displacements and rotations, and their corresponding velocities and accelerations are derived in the X vector.

In the present study, shell elements with six degrees of freedom (DOFs) per node have been used in Abaqus modeling. In the data transfer process, first, the node numbers are converted into a system of global DOFs. The sparse format of the mass and stiffness matrices extracted from Abaqus includes a size of $R \times 5$, in which R is the number of nonzero components of the global stiffness matrix. The quantities involved in the 5th column of these matrices are row node label and its DOF, column node label and its DOF, and stiffness value, as well. In the import operation, the mentioned format is converted to a full one according to the DOFs generated into MATLAB. It should be noted except for two DOFs, namely displacement in the z -direction and the rotation about the x -axis, the other DOFs are negligible. Thus, it is possible to use strain modal identification theory.

4. STRAIN-BASED IDENTIFICATION TECHNIQUE

To apply the modal identification technique, the structural model is assumed linear in the intact and delaminated laminates. Analyzing a composite laminate under impact loading shows that two DOFs, translation along the thickness and rotation along the width, out of six DOFs are considerable. Thus, the strain identification theory applied to the Euler-Bernoulli beam with two DOFs per node may be utilized. According to this theory, under the impact loading, the average strain available in a set of several sequential elements, n , with length L_n may be calculated as follows:

$$\bar{\varepsilon}_n = (h_n/L_n)(\psi_y^i(t) - \psi_y^j(t)) \quad (7)$$

where h_n is the distance of the location at which average strain is calculated from beam's neutral axis; $\psi_y^i(t)$ and $\psi_y^j(t)$ obtained in sections 2 and 3 are the rotational DOFs of the first node of the first element, i , and the last node of the last element, j , with respect to time, t . It should be noted that several elements (element set) represent a sensor having a gauge length, L_n .

Impact load as input data at one point and average strains calculated using Equation (7) as output data at nodes along the laminate length are used to extract strain frequency functions. This process may be repeated for other input points. Therefore, the average-strain frequency response functions (SFRF) within the frequency domain between the input data, f_z , applied at point q and each individual output data $\bar{\varepsilon}_n$ may be achieved by:

$$H_{nq}^{\bar{\varepsilon}}(\omega) = \bar{\varepsilon}_n(\omega) / f_z^q(\omega) \quad (8)$$

To calculate SFRFs, adding some noise, $N(\omega)$, into the output, $\hat{\varepsilon}_n(\omega) = H_{nq}^{\bar{\varepsilon}}(\omega) \cdot f_z^q(\omega) + N(\omega)$, post multiplying by the conjugate transpose of the input, f_z^{q*} , and taking expectations, Equation (8) is converted into:

$${}^1H_{nq}^{\bar{\varepsilon}}(\omega) = \frac{E[\hat{\varepsilon}_n(\omega) \cdot f_z^{q*}(\omega)]}{E[f_z^q(\omega) \cdot f_z^{q*}(\omega)]} = \frac{S_{nq}(\omega)}{S_{qq}(\omega)} \quad (9)$$

where E and $*$ represent expectation and conjugate transpose. $S_{nq}(\omega)$ and $S_{qq}(\omega)$ denote the cross-spectral density of the input and output and the auto-spectral density of the input, respectively. The cross-spectral density is the Fourier transform of the cross-correlation function. It is obtained an SFRF matrix with the size of (number of output points) \times (number of input points), in which each component is a function of frequency.

To extract strain-based modal parameters using the SFRF matrix, two methods are examined in the present study. In the first method, SFRF matrix is directly employed for calculating strain-based modal responses of the laminate through selecting and connecting the maximum values within each column of the matrix [9]. In the second method, the single value decomposition (SVD) technique is applied to the SFRF matrix relying on the complex modal indicator function (CMIF). CMIF diagram may be used to identify the actual number and form of modal responses. CMIF plots eigenvalues on a log magnitude scale versus frequencies. The singular value decomposition of the strain frequency function matrix, ${}^1H_{nq}^{\bar{\varepsilon}}(\omega)$, is given as follows:

$${}^1H_{nq}^{\bar{\varepsilon}}(\omega) = USV^H \quad (10)$$

where U and V are unitary matrices; S is a diagonal matrix containing real singular values; and H stands for complex conjugate transpose. In other words, the S components are the singular values (natural frequencies), and their associated singular vectors (mode shapes) are placed in the U and V matrices. Therefore, this section provides strain-based frequency and modal shape components.

5. DELAMINATION IDENTIFICATION INDICATORS

Delamination identification indicators in composites highlight the delamination location involving the first and final nodes of the delaminated length, i.e., the delaminated element, and the interface position. For detecting the longitudinal location of delamination, the following strain modal shape based indicators are employed to highlight delaminated elements.

1. The strain modal shape variation (SMSV):

$$SMSV = \max \left(\sum_{j=1}^{\infty} |{}^D\phi_{nk}^{\bar{\epsilon}} - {}^I\phi_{nk}^{\bar{\epsilon}}| \right) \quad (11)$$

where D, I, k and n stand for delaminated, intact, mode number and element number, respectively. ${}^I\phi^{\bar{\epsilon}}$ and ${}^D\phi^{\bar{\epsilon}}$ are the strain modal shapes in intact and delaminated laminates extracted in section 4.

2. The strain modal shape curvature variation (SMSCV):

$$SMSCV = \max \left(\sum_{j=1}^{\infty} |{}^D\phi_{nk}^{\prime\prime\bar{\epsilon}} - {}^I\phi_{nk}^{\prime\prime\bar{\epsilon}}| \right) \quad (12)$$

where $\phi_n^{\prime\prime} = (\phi_{n+1} - 2\phi_n + \phi_{n-1}) / L_n^2$.

6. NUMERICAL EXAMPLES

The first example tries to demonstrate the performance of the strain-based delamination identification technique. The second one compares displacement-based results to those of strain. When $0 < t < 1$ s, the impact loading is 1000 N at $t = 0.1$ s; otherwise it is zero.

6. 1. Clamped-free Supported Cross-ply Laminate

The first example is assumed to be an eight-layer cross-ply $[0=90]_{2s}$ laminate with clamped-free supports [13]. Figure 2 (a) shows its dimensions, $127\text{mm} \times 12.7\text{mm} \times 1.016\text{mm}$, and delamination cases with length of 25.4mm . The characteristics of the material are: $E_{11} = 134.49\text{GPa}$, $E_{22} = 10.34\text{GPa}$, $\nu_{12} = 0.33$, $G_{12} = 5.00\text{GPa}$, $\rho = 1500 \text{ kg/m}^3$. To investigate the effect of different delamination locations on the frequency parameters, lengthwise delamination is located at the middle and free end of the laminate in two cases of near and far from the laminate's surface, i.e., near- and far-surface. Delamination cases 1 and 3 at the middle interface and cases 2 and 4 at the topmost interface are located.

6. 1. 1. Model Verification For the illustration of the convergence process of solution, the von misses strain on the laminate's middle path is plotted in Figure 3. Accordingly, the element size of 30×4 is selected. The laminate for the FE modeling is therefore divided into thirty elements in the longitudinal direction, in which every three elements represents a sensor set with the gauge length $L_n = 12.7\text{mm}$, as shown in Figure 2 (b).

For verification of SFRF-based natural frequencies, the frequencies of the first four flexural modes extracted from average SFRFs obtained by applying the Bathe method are compared with those predicted from Abaqus for the intact laminate, as listed in Table 1.

Average errors are calculated based on the reference data [13]. The SFRF-based results utilize the average

strains of several elements instead of exact strains of those elements. Despite the approximations, they show good predictions. To verify the connection modes, each delamination case is analyzed with both constrained and free mode.

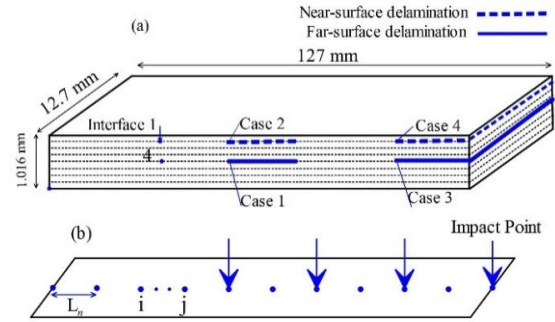


Figure 2. (a) Geometrical dimensions and delamination locations; (b) Middle path

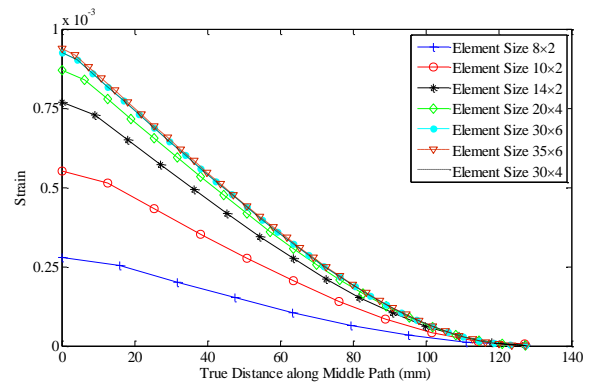


Figure 3. Strain's convergence along the middle path

TABLE 1. Four modal frequencies of the intact and delaminated laminate (in Hz)

Intact laminate		Mode 1	Mode 2	Mode 3	Mode 4
Abaqus (Error percentage)		82.156 (0.14)	515.32 (0.016)	1446.3 (0.64)	2845.3 (-)
SFRF (Error percentage)		83.58 (1.84)	511.44 (0.77)	1350.25 (6.4)	2287.5 (6 (-))
Delaminated laminate		Mode 1	Mode 2	Mode 3	Mode 4
Case 1	Free	78.362	447.21	1328.1	2635.5
Case 1	Constrained	78.476	447.47	1368	2643.8
Case 2	Free	78.383	444.36	1407.9	2337.4
Case 2	Constrained	78.38	444.58	1408.5	2659.2
Case 3	Free	82.117	508.93	1099.7	1356.2
Case 3	Constrained	82.131	511.06	1382.7	2631.7
Case 4	Free	81.986	312.44	526.56	1414.9
Case 4	Constrained	82.14	512.51	1399	2674.2

According to Table 1, the free mode for simulating Ccases 2, 3 and 4, particularly in higher modes, unrealistically underestimates the frequencies of the delaminated laminate. Therefore, the constrained mode is hereafter employed to simulate connection between the sub-laminates. Furthermore, two cases 1 and 4, respectively having the most and the least effects on frequencies, as seen in Table 1, are selected for further study.

Changes appeared in modal responses due to delamination are also a function of the interface location in addition to its longitudinal location. To investigate the interface of delamination, the frequency shifts between the intact and delaminated laminate, i.e., $\omega_I - \omega_D$, for each interface and case are calculated based on rotations transferred to each interface. Percentile means of interfaces 1-4 are 0.92, 1.04, 1.13, **1.16** for case 1 and **0.45**, 0.42, 0.32, 0.18 for Case 4, respectively. They show that interface 4 and interface 1 are of the highest rate of frequency shifts for case 1 and case 4, respectively. The predicted interfaces are in complete agreement with actual delaminated interfaces, as shown in Figure 2 (a).

6.1.2. Delamination Identification Process The results for the middle interface of the laminate are used for delamination identification. For dynamic analysis, two matrices of mass and stiffness are validated by the frequency values (section 6.1.1). Applying impact loading at points specified in Figure 2 (b), the responses at all points can be extracted. Rotations used in Eq. 7 obtained by the Bathe method under impact are validated with those obtained from Abaqus employing implicit dynamic analysis. Using these two rotation sets, average strains in Eq. 7 are obtained. In addition, SFRFs in Eq. 9 are estimated from the impact load and the two average-strain datasets. For illustration purpose, the corresponding average strains and SFRFs obtained from rotations of MATLAB and Abaqus are depicted in Figures 4 (a) and 4(b), respectively. Totally, there are 4 input and 11 output channels along the longitudinal direction with uniform interspacing; thus, the dimensions of the SFRF matrix estimated are 11×4 at each frequency line.

To extract average-strain modal parameters, two methods are examined in the present study. The first one is using direct SFRFs by selecting and connecting the peaks (Figure 5 shows only two out of ten subfigures for one impact point), and the second one is performing the SVD technique on the SFRF matrix relying on CMIF. According to Figure 5, magnitudes of four first structural modes are denoted by picking and connecting the circles on the curve peaks at each natural frequency. SVD-based modal parameters are more reliable since the direct SFRF method is not coherent at estimating the location of the third and fourth modes. As a result, the

SVD technique is applied in subsequent evaluations. Applying the SVD technique to the total SFRF matrix (11×4) at each discrete frequency point, extracting CMIF plots, and peak picking the singular values

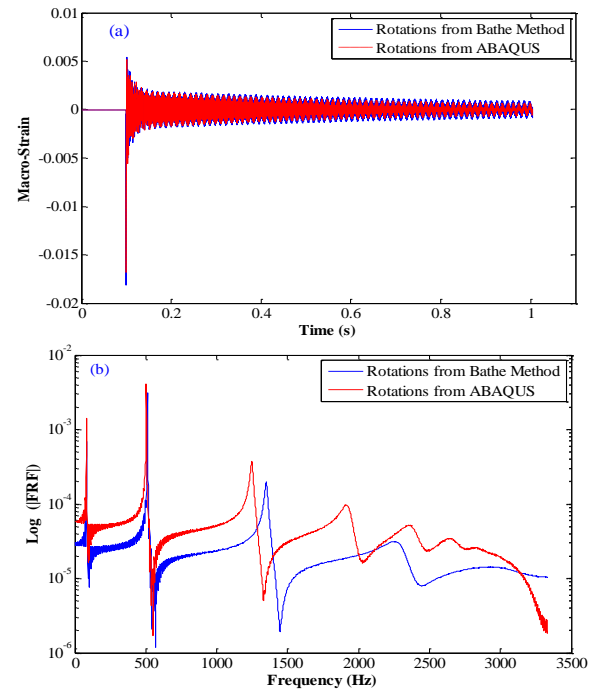


Figure 4. The intact laminate: (a) average (macro) strains and; (b) associated SFRFs

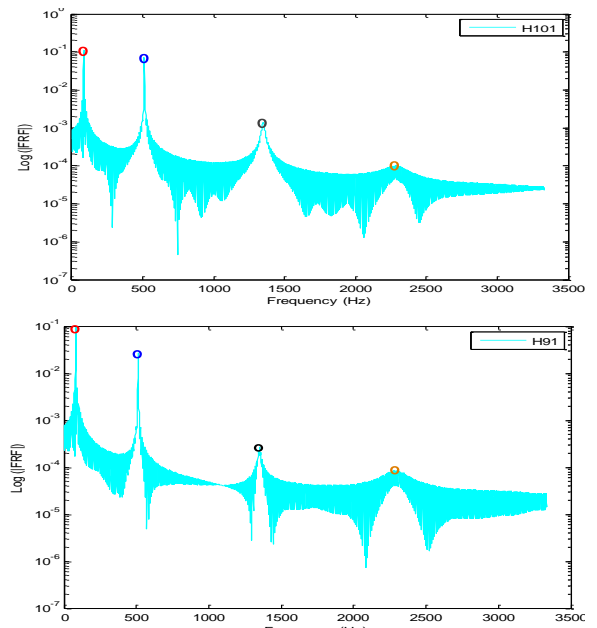


Figure 5. Connecting peaks in typical SFRFs of the intact laminate extracted from MATLAB

(Equation (10)), the natural frequencies and corresponding mode shapes can be obtained. CMIF plots (not shown for brevity), in which the number of both curves and impacting points are four, clear that the accuracies of the modal parameters with 4 impact and 1 impact loads are approximately the same. Thus, the results hereafter are extracted only under one impact.

Next, mode shapes of the delaminated laminate including cases 1 and 4 are obtained and compared to those of the intact laminate extracted from the Bathe method applying the SVD technique on SFRFs and also extracted from Abaqus, i.e., exact mode shapes. Figures 6 and 7 show the normalized strain mode shapes for Cases 1 and 4, respectively. There is a good agreement between mode shapes of the intact laminate extracted from SFRF and exact ones extracted from Abaqus. As depicted in Figure 6, significant discontinuities available at element-set numbers five and six show the delamination location. Even without further processing, delaminated elements are identified. However, the damage locations in Figure 7, namely element-set numbers nine and ten, are not as clear as those in case 1. The reason is that the delamination regions at the free end of the laminate do not considerably affect the modal responses. It has also been proved in Table 1 that frequencies in case 4 are the least affected ones by delamination. Thus, to highlight the delamination locations, two damage indicators given in Equations (11) and (12) are applied to the identified strain modal shapes (Figures 6 and 7). For brevity, only the SMSCV indicator results are provided in Figure 8, in which the exact delamination locations are clearly identified.

6. 2. Clamped-supported Angle-ply Laminate

As shown in Figure 10 (a), the laminate is composed of the six-layer glass fiber lamina with epoxy resin laminated in $[0/+45/-45]_S$ lay-up of dimensions $500\text{mm} \times 100\text{mm} \times 4\text{mm}$ [7]. Both ends are clamped. The material properties are: $E_{11}=25.1\text{GPa}$, $E_{22}=E_{33}=10.2\text{GPa}$, $\nu_{12}=\nu_{13}=0.37$, $\nu_{23}=0.41$, $G_{12}=3.6\text{GPa}$.

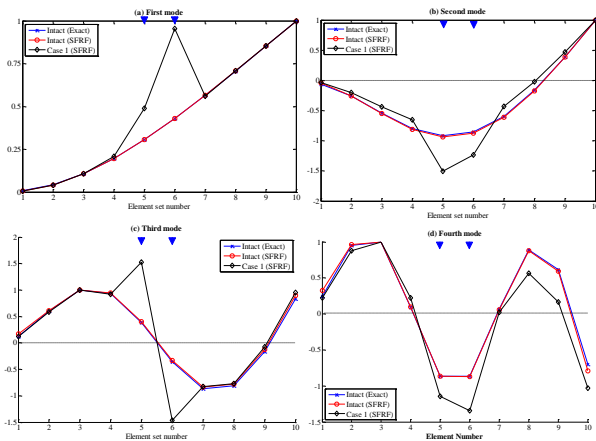


Figure 6. Identified strain mode shapes for Case 1

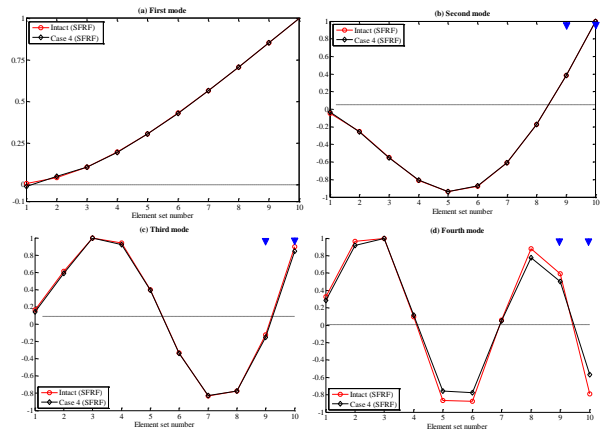


Figure 7. Identified strain mode shapes for case 4

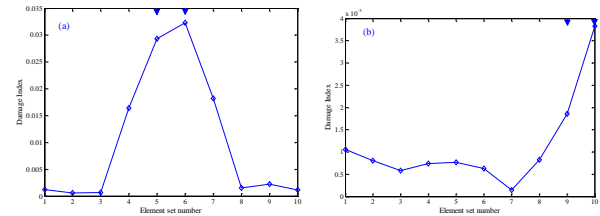


Figure 8. The SMSCV indicator for delamination detection: (a) Case 1; (b) Case 4

Delamination cases 1 and 2 with dimensions of $50\text{mm} \times 100\text{mm}$ and $25\text{mm} \times 100\text{mm}$ are located based on the least effective location on frequency parameters. Accordingly, delamination cases are assumed at the same axial location and interface but two different delamination lengths. A mesh with dimensions of 40×8 is utilized.

6. 2. 1. Displacement- and Strain-based Delamination Identification

For the delamination identification process, rotations used in Equation (7) are extracted at the first and last nodes of a two-element set, namely a total of twenty element sets in which each set represents one sensor with the gauge length of 25mm . The first four frequencies for the intact laminate including those of SFRFs using the Bathe method and of the frequency analysis in Abaqus are 51.5 (6.78), 137.5 (6.26), 250 (2.29), 361 (18.61) and 48.03 (6.13), 128.89 (8.78), 255.73 (7.94), 428.18 (7.11), respectively. The percentage errors are provided in the parenthesis. The SFRF results show good agreement to the experimental results except for mode number four for which less value than the experimental one is predicted. Figure 9 (b) illustrates five CMIF curves in which the loading application point is varied. Except for black CMIF curve, which is corresponding to the impact loading, applied at the laminate’s center, all other curves clearly demonstrate the first four frequencies.

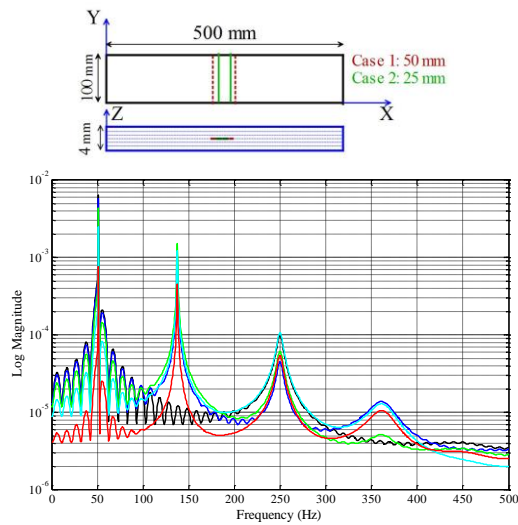


Figure 9. (a) Laminate geometry and delamination cases; (b) The CMIF plots of the SFRF matrix for the intact laminate under impact at different locations

Accordingly, impact loading is used only at one point for the delaminated cases, as the modal parameters are approximately the same.

Assuming the interface in this example is known, it is emphasized on detecting the delamination location. To this end, the strain modal parameters including frequencies and mode shapes are obtained from CMIF plots in the intact and delaminated situations. After identifying the mode shapes, strain mode shapes in delaminated cases 1 and 2 are overlapped with those of the intact laminate. Besides, the associated displacement mode shapes are plotted along with those related to the average strain. For illustration, Figure 10 shows the result of the delaminated case 1, in which the blue arrows on the top of the figure show the exact delaminated elements. It is clearly observed that the displacement mode shapes in the delaminated case show no visible difference compared with those in the intact laminate. They are apparently the same, while the strain mode shapes demonstrate considerable differences in the delaminated elements compared to the intact elements. It is notable that discontinuities in places of delamination, namely element sets ten and eleven, predict the delaminated elements without any further evaluations even without referring to the base data of the intact laminate. For more clarity, the mentioned indicators for damage detection are calculated in delaminated cases 1 and 2, as plotted in Figure 11.

The blue triangles show the exact delaminated elements. In delaminated case 1, the delamination intensity or surface is twice as much as that in the delaminated case 2. Having a look at the maximum amounts of damage index in element set numbers ten and eleven in Figure 11, it can be concluded that

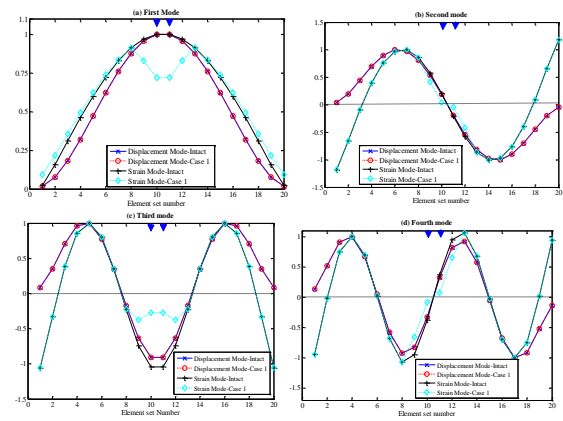


Figure 10. Performance of strain mode shapes compared with displacement mode shapes

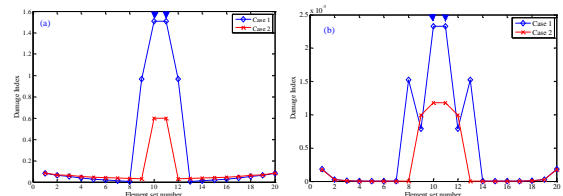


Figure 11. Damage detection indicators: (a) SMSV indicator and (b) SMSCV indicator

damage index value in the delaminated elements in case 1 is more than twice that of case 2. Scientifically speaking, measuring strain as a global and local response of the structure instead of displacement must be paid attention.

7. CONCLUSIONS

An SFRF-based technique embedded into damage indicators has been utilized to identify delamination with respect to strain measurements. The following conclusions can be drawn:

1. The constrained mode employing contact elements between the upper and lower sublaminates has generally shown better accuracy to predict the modal parameters than the free mode.
2. Modal parameters extracted from the SVD technique compared to those of the direct SFRF matrix are more reliable since this technique predicts higher modal parameters to be more consistent.
3. CMIF plots of the SFRF matrix resulted from impact loading applied at different longitudinal locations illustrate the impact application point has considerable influence on the natural frequencies to be appeared on the plot. Nonetheless, one impacted point compared to a set of several impacted points embedded into the SFRF matrix seems to be sufficient.

4. There is a good agreement between the exact strain modal parameters and those of the average strain of the FRF matrix in the intact and delaminated cases. Places at which the delamination location is not clearly apparent from some strain modal shapes in the delaminated cases, some indicators highlight the delaminated elements, and the delamination intensity is also approximated.

5. Different levels of noise are added to data fed into the proposed technique to simulate the environmental noise. The delamination identification technique also displays to be efficient under noise.

6. In spite of the efficiency of strain modal shapeshifts, displacement modal parameters show no clear change in the delaminated regions compared with the intact regions.

8. REFERENCES

1. Wang, Y. and Wu, Q., "Experimental detection of composite delamination damage based on ultrasonic infrared thermography", *International Journal of Engineering, Transactions B: Applications*, Vol. 27, No. 11, (2014), 1723–1730.
2. Saeedifar, M., Najafabadi, M. A., Zarouchas, D., Toudeshky, H. H. and Jalalvand, M., "Barely visible impact damage assessment in laminated composites using acoustic emission", *Composites Part B: Engineering*, Vol. 152, (2018), 180-192.
3. Singh, S. and Angra, S., "Flexural and impact properties of stainless steel based glass fibre reinforced fibre metal laminate under hygrothermal conditioning", *International Journal of Engineering, Transactions A: Basics*, Vol. 31, No. 1, (2018), 164-172.
4. Zhang, Z., Shankar, K., Ray, T., Morozov, E. V., and Tahtali, M., "Vibration-based inverse algorithms for detection of delamination in composites", *Composite Structures*, Vol. 102, (2013), 226–236.
5. Yang, C. and Oyadiji, S. O., "Detection of delamination in composite beams using frequency deviations due to concentrated mass loading", *Composite Structures*, Vol. 146, (2016), 1-13.
6. Hassan, A., El-Wazery, M., and Zoalfakar, Sh., "Health monitoring of welded steel pipes by vibration analysis", *International Journal of Engineering, Transactions C: Aspects*, Vol. 28, No. 12, (2015), 1782–1789.
7. Chandrashekhar, M. and Ganguli, R., "Damage assessment of composite plate structures with material and measurement uncertainty", *Mechanical Systems and Signal Processing*, Vol. 75, (2016), 75–93.
8. Li, S. and Wu, Z., "Modal analysis on macro-strain measurements from distributed long-gage fiber optic sensors", *Journal of Intelligent Material Systems and Structures*, Vol. 19, No. 8, (2008), 937–946.
9. Zhang, J., Guo, S., Wu, Z., and Zhang, Q., "Structural identification and damage detection through long-gauge strain measurements", *Engineering Structures*, Vol. 99, (2015), 173–183.
10. Barbero, E. J., "Finite element analysis of composite materials using AbaqusTM", CRC press, (2013).
11. Della, C. N. and Shu, D., "Vibration of delaminated composite laminates: A review", *Applied Mechanics Reviews*, Vol. 60, No. 1, (2007), 1–20.
12. Askaripour, Kh. and Fadaee, M. J., "Modification of an implicit approach based on nonstandard rules for structural dynamics analysis", *Mechanics Based Design of Structures and Machines*, (2018), 1–17.
13. Shen, M.-H. and Grady, J., "Free vibrations of delaminated beams", *AIAA Journal*, Vol. 30, No. 5, (1992), 1361–1370.

Diagnosis of Delaminated Composites Using Post-processed Strain Measurements under Impact Loading

K. Askaripour, M. J. Fadaee

Department of Civil Engineering, Shahid Bahonar University of Kerman, Kerman, Iran

PAPER INFO

چکیده

Paper history:

Received 20 November 2018

Received in revised form 21 December 2018

Accepted 03 January 2019

Keywords:

Composite

Delamination Identification

Dynamic Strain

Impact

پدیده نامرئی تورق که دارای اثر مخربی روی خواص مکانیکی لمینیت‌های کامپوزیت است به طور مکرر تحت بارگذاری ضربه‌ای رخ می‌دهد. در مطالعه فعلی، با شبیه‌سازی عملکرد سنسورهای فیبری شبکه براگ با طول زیاد، کرنش‌های متوسط ناشی از ضربه در کامپوزیت‌های لایه‌ای برای توسعه تکنیک شناسایی تورق استفاده می‌شوند. ابتدا، پارامترهای مودال مبتنی بر کرنش از توابع پاسخ فرکانسی با استفاده از دو روش مختلف استخراج می‌شوند. سپس، این پارامترها در شاخص‌های شناسایی آسیب مختلف بکار می‌روند. بعد از آن، حضور، موقعیت و شدت تورق معرفی شده در موقعیت‌های با کمترین تاثیر روی تغییرات مودال شناسایی می‌شوند. نتایج مثال‌های عددی مختلف بیانگر کارایی قابل توجه سنجش‌های کرنش متوسط برای شناسایی کامپوزیت‌های متورق شده هستند.

doi:10.5829/ije.2019.32.01a.07